Engineering Mixing Properties of Fluids by Spatial Modulations

Abid Ali◉ and Hiroki Saito◉

Department of Engineering Science, University of Electro-Communications, Tokyo 182-8585, Japan

We propose a method to change the effective interaction between two fluids by modulation of their local density distributions with external periodic potentials, whereby the mixing properties can be controlled. This method is applied to a mixture of dilute bosonic gases, and binodal and spinodal curves emerge in the phase diagram. Spinodal decomposition into a mixed-bubble state becomes possible, in which one of the coexisting phases has a finite mixing ratio. A metastable mixture is also realized, which undergoes phase separation via nucleation.

A binary mixture becomes thermodynamically unstable and separates into two stable phases, when a control parameter, such as temperature, is quenched across the critical point. Such spontaneous phase separation of mixtures is known as spinodal decomposition [1–4]. On the other hand, if the binary mixture is prepared in a metastable state, finite perturbation is required for nucleation and growth to proceed to phase separation [5–7]. Spinodal decomposition and nucleation are the two major mechanisms responsible for phase separation in multicomponent systems. The boundary between the spinodal and nucleation regions in the phase diagram is called a spinodal curve, and that between the nucleation and stable regions is called a binodal curve. These three regions appear when the free energy has both concave and convex shapes as a function of the mixing ratio.

The separated and mixed fluids have different free energies, since the energy and entropy are changed by mixing. Here we focus on the mixing energy, which is the energy difference between separated and mixed fluids. The mixing energy is determined by the interaction between constituent particles of two fluids, which is generally difficult to control. The purpose of this Letter is to alter the mixing energy by a simple method—modulation of the local density distributions by external periodic potentials, whereby mixing properties of fluids are controlled. Let us consider a mixing energy $E_{\text{mix}}[n_1(\boldsymbol{r}), n_2(\boldsymbol{r})]$, which is dependent on the density distributions $n_1(\boldsymbol{r})$ and $n_2(\boldsymbol{r})$ of components 1 and 2. If we apply external potentials that locally modulate the density distributions, the local overlap between $n_1(\boldsymbol{r})$ and $n_2(\boldsymbol{r})$ is modulated. On a scale much larger than the modulation wavelength, the effective mixing energy is given by the spatial average $\langle E_{\text{mix}}[n_1(\boldsymbol{r}), n_2(\boldsymbol{r})]\rangle_{\boldsymbol{r}}$. Therefore, the global mixing energy can be changed, which alters the global mixing properties.

We apply this method to a binary mixture of Bose-Einstein condensates (BECs) of ultracold gases [8–15], which is a clean and highly controllable system. In this system, external periodic potentials can be easily generated

and precisely controlled using optical lattices [16], making the system suitable for the present purpose. In a mixture of dilute BECs, in which simple mean-field theory is applicable, the mixing property for a homogeneous system is trivial, i.e., the mixture is either stable or unstable against phase separation, irrespective of the mixing ratio, and there are no binodal and spinodal curves in the phase diagram (with respect to the mixing ratio). It was recently predicted that a beyond-mean-field effect [17] can modify the energy curve, and an interesting separated phase (mixed-bubble state) is possible [18,19], in which one of coexisting phases has a finite mixing ratio. Liquid-gas coexistence in this system was also studied recently [20–22].

Here we show that binodal and spinodal physics emerge in a binary mixture of BECs simply by applying a component-dependent periodic external potential, which modulates the mixing energy as a function of the mixing ratio. As a result, spinodal decomposition into the mixed-bubble state becomes possible without beyond-mean-field effects. Moreover, the mixture can be brought to a metastable state, in which a finite perturbation is required to cross the energy barrier against phase separation, which leads to nucleation and growth toward the separated phase.

We consider a binary mixture of dilute Bose gases at zero temperature, which can be described by the macroscopic wave functions Ψ_1 and Ψ_2 in the mean-field approximation. The energy of the system can be written as [23,24]

$$E = \int d\boldsymbol{r} \left[\sum_{j=1}^{2} \left(-\frac{\hbar^2}{2m} \Psi_j^* \nabla^2 \Psi_j + V_j |\Psi_j|^2 + \frac{g_{jj}}{2} |\Psi_j|^4 \right) + g_{12} |\Psi_1|^2 |\Psi_2|^2 \right], \quad (1)$$

where m is the atomic mass. The wave function $\Psi_j(\boldsymbol{r}, t)$ satisfies $\int d\boldsymbol{r} |\Psi_j(\boldsymbol{r}, t)|^2 = N_j$, where N_j is the number of atoms for component j. The interaction coefficients are defined as $g_{jj'} = 4\pi\hbar^2 a_{jj'}/m$, where $a_{jj'}$ is the s-wave

scattering length between components j and j'. In the present work, the atomic interactions are repulsive with positive scattering lengths, $g_{ij} > 0$. We consider a situation in which a periodic potential $V_j(\mathbf{r}) = U_j \cos^2(kx)$ is applied to the system, where $U_1 > 0$ and $U_2 < 0$ [see Fig. 1(a)]. Such a component-dependent periodic potential can be
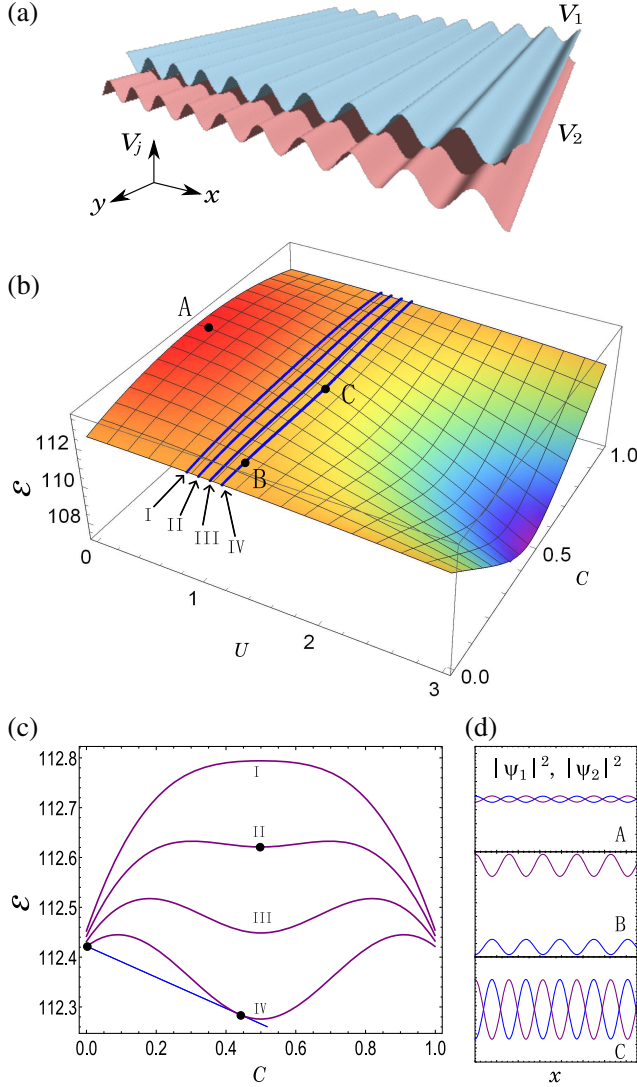

FIG. 1. (a) Schematic illustration of external periodic potentials $V_1 = U \cos^2(kx)$ for component 1 and $V_2 = -U \cos^2(kx)$ for component 2. (b) Variational energy ε in Eq. (3) as a function of potential strength U and composition C, where variational parameters a_1 and a_2 are selected to minimize ε. The curves I, II, III, and IV correspond to $U = 0.9$, 1, 1.1, and 1.2, respectively, which are shown in (c) as a function of C. The density distributions $|\Psi_1|^2$ and $|\Psi_2|^2$ are shown in (d), where panels A, B, and C correspond to the points marked in (b). The tangential line and circles on curves IV and II in (c) correspond to the mixed-bubble state and metastable state, respectively, which are presented in Figs. 2 and 3. The interaction parameters are $g_{11} = g_{22} \equiv g = 15$ and $g_{12} = 15.3$.

produced by laser beams with a selected wave number and polarization [25–32].

For a homogeneous system without an optical lattice, the energy density is given by $\varepsilon = (g_{11} n_1^2 + g_{22} n_2^2)/2 + g_{12} n_1 n_2$, whose curvature $g_{11} g_{22} - g_{12}^2$ is constant with respect to the uniform densities n_1 and n_2. Therefore, there are only two ways to minimize $\omega \equiv \varepsilon - \mu_1 n_1 - \mu_2 n_2$, where μ_j are the chemical potentials. For a positive curvature, there can be a single minimum with nonzero n_1 and n_2, which corresponds to the uniformly mixed state. For a negative curvature and appropriate μ_j, ω can be simultaneously minimized at the two points $n_1 = 0$ (with $n_2 \neq 0$) and $n_2 = 0$ (with $n_1 \neq 0$), which corresponds to the separated state. Thus, the phase diagram is trivial: the ground state is either the uniformly mixed state or the totally separated state, which is determined only by the sign of the curvature $g_{11} g_{22} - g_{12}^2$, and is independent of the mixing ratio N_1/N_2. In the presence of component-dependent periodic external potentials, as shown in Fig. 1(a), the density distributions $|\Psi_1(\mathbf{r})|^2$ and $|\Psi_2(\mathbf{r})|^2$ are modulated [see Fig. 1(d)], and their local overlap can be decreased. As a result, the global mixing energy of the system is changed, and the phase diagram will be altered.

To present this clearly, we employ a simple variational method. The wave function is approximated as

$$\Psi_j(\mathbf{r}) = \sqrt{n_j[1 + a_j \cos(2kx)]}, \qquad (2)$$

where a_j is the real variational parameter satisfying $|a_j| < 1$. Substituting the variational wave function $\Psi_j(\mathbf{r})$ into the energy of the system in Eq. (1) gives

$$\varepsilon \equiv \frac{E}{N} = \sum_{j=1}^{2} \left[\frac{n_j}{2} \left(1 - \sqrt{1 - a_j^2} \right) + \frac{U_j n_j a_j}{4} \right.$$
$$\left. + \frac{g n_j^2}{2} \left(1 + \frac{a_j^2}{2} \right) \right] + g_{12} n_1 n_2 \left(1 + \frac{a_1 a_2}{2} \right), \qquad (3)$$

where $g_{11} = g_{22} \equiv g$ is assumed and $N = N_1 + N_2$. In Eq. (3), all the quantities are dimensionless (see the Supplemental Material [33] for details). It is also assumed that $|g_{12} - g| \ll g$, which maintains the total density $|\Psi_1|^2 + |\Psi_2|^2$ to be almost uniform. In this case, n_1 and n_2 can be parametrized by the composition C as $n_1 = C$ and $n_2 = 1 - C$ with $0 \leq C \leq 1$. In the following, we also assume $U_1 = -U_2 \equiv U$. These assumptions are only to reduce the number of parameters and are not crucial for the main results obtained later.

Figures 1(b) and 1(c) show the variational energy ε as a function of the potential strength U and composition C, where ε has been minimized with respect to the variational parameters a_j. For a small value of U, the energy curve is concave (curve I), since the interaction parameters satisfy $g_{11} g_{22} - g_{12}^2 < 0$. Therefore, $C = 0$ and 1 minimize the

energy, which indicates that the mixture is energetically unstable against phase separation. As the value of U is increased, the energy curve is modified, and the metastable state appears for $U = 1$ (curve II). For $U \gtrsim 1.1$, the energy around $C = 0.5$ decreases and goes below those for $C = 0$ and 1 (curves III and IV). It should be noted that such a concave-convex shape of ε is due to the nonlinear dependence of Eq. (3) on C and U through the optimization of a_j (see the Appendix for details), yielding the nontrivial mixing properties. This effect therefore cannot be described by the tight-binding model [37], which has been used in previous studies on a two-component BEC in an optical lattice [38–47].

From the energy curves in Fig. 1(c), the energetic stability of the state against phase separation can be understood in a diagrammatic manner [48]. Let us consider a point on an energy curve $[C_0, \varepsilon(C_0)]$, and consider a situation in which the entire system is occupied by this state. Although this state is alternately modulated in the x direction, as shown in Fig. 1(d), from a coarse-grained point of view on a scale much larger than the modulation wavelength, the two components are uniformly mixed on average, and we refer to this state as a "globally mixed state." Suppose that this phase with C_0 separates into two phases with $C_+(> C_0)$ and $C_-(< C_0)$. It can be shown that the energy of the separated state is given by $\varepsilon_{\text{sep}} = [\varepsilon(C_-)(C_+ - C_0) + \varepsilon(C_+)(C_0 - C_-)]/(C_+ - C_-)$ (See the Supplemental Material [33]), which corresponds to the intersection point between the vertical line $C = C_0$ and the line connecting the two points $[C_+, \varepsilon(C_+)]$ and $[C_-, \varepsilon(C_-)]$. When this energy ε_{sep} is larger (smaller) than $\varepsilon(C_0)$, the globally mixed state with C_0 is energetically stable (unstable) against phase separation into two phases with $C_\pm$. Thus, within the region of $\partial^2 \varepsilon / \partial C^2 < 0$, the globally mixed state is always unstable against phase separation. If $\partial^2 \varepsilon / \partial C^2 > 0$ and there exist $C_\pm$ such that $\varepsilon_{\text{sep}} < \varepsilon(C_0)$, then the globally mixed state is metastable.

For $U = 1.2$, the energy curve with respect to C acquires a concave-convex shape, as shown by the curve IV in Fig. 1(c). In this case, the globally mixed state for, e.g., $C = 0.1$ is unstable against phase separation. From the above consideration, the most stable (lowest-energy) separated pair of phases is given by the tangential line shown in Fig. 1(c), which gives $C_- = 0$ and $C_+ \simeq 0.426$ (two circles on the line). This indicates that if the globally mixed state with $C = 0.1$ is prepared, it separates into two phases; one phase is occupied by only component 2 ($C_- = 0$), and the other phase is occupied by both components ($C_+ \simeq 0.426$). This separated state is referred to as a mixed-bubble state, and was first predicted in Ref. [18], in which the concave-convex energy curve is caused by the beyond-mean-field effect. Here, the mixed-bubble state emerged even in a system described by simple mean-field theory, where the concave-convex energy curve arises from the local modulation.

To confirm the results of the variational analysis, we numerically solve the coupled Gross-Pitaevskii (GP) equation,

$$i\frac{\partial \Psi_j}{\partial t} = \left(-\frac{\nabla^2}{2} + V_j + g|\Psi_j|^2 + g_{12}|\Psi_{j'}|^2 \right)\Psi_j, \quad (4)$$

where $(j, j') = (1, 2)$ and $(2,1)$. Note that the results in Fig. 1 are not dependent on the dimensionality, and here we consider a two-dimensional system. The GP equation is integrated using the split-operator pseudospectral method [49] with the periodic boundary condition, where the system is discretized into a mesh with $dx = dy = 2\pi/64$ and the time step is typically $dt = 0.001$.

First, we solve the imaginary-time evolution of Eq. (4) to obtain the ground state, in which i on the left-hand side is replaced by -1. Figure 2(a) shows the density distributions, $|\Psi_1|^2$ and $|\Psi_2|^2$, of the ground state for $U = 1.2$ and $C = 0.1$. As expected from the variational results, the ground state is the mixed-bubble state, which contains a single bubble of a mixed phase surrounded by component 2. Equating the typical energy ~ 0.1 relevant to the phase
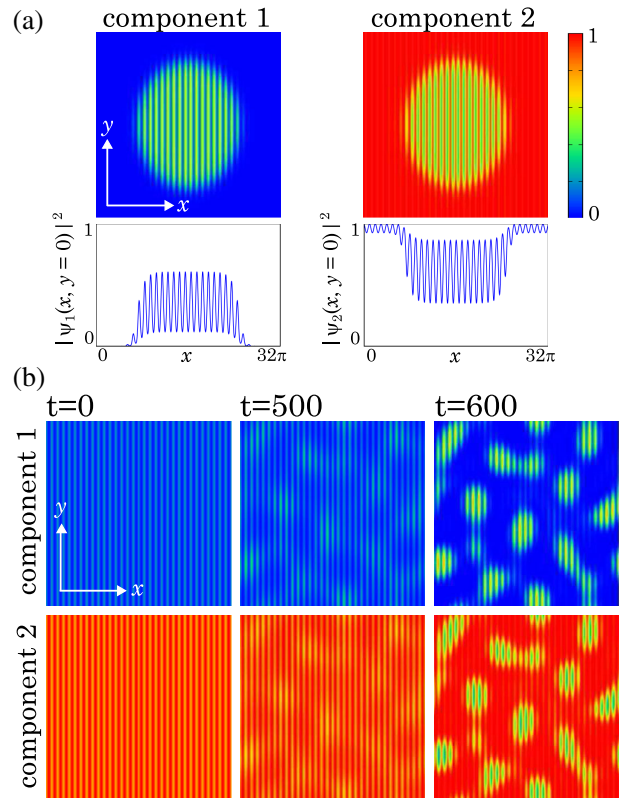

FIG. 2. Mixed-bubble state for $C = 0.1$, $g = 15$, $g_{12} = 15.3$, and $U = 1.2$, which corresponds to the energy curve IV in Fig. 1(c). (a) Ground state obtained by solving the GP equation. (b) Dynamics of the mixed-bubble formation. The initial state is the ground state for $g = g_{12} = 15$. At $t = 0$, g_{12} is suddenly changed to 15.3. See the Supplemental Material [33] for a movie of the dynamics. The size of each panel is $(32\pi)^2$.

separation [the energy difference along the curve IV in Fig. 1(c)] with $(2\pi/\xi_s)^2/2$, we can estimate the quasispin healing length $\xi_s \sim 4\pi$, which is consistent with the interface width between the two phases in Fig. 2(a). The bubble in Fig. 2(a) is slightly elongated in the y direction, which implies that the interfacial tension between the two phases is anisotropic due to the periodic potential in the x direction. Figure 2(b) shows the real-time evolution, in which the initial state is the ground state for $g = g_{12} = 15$ and $C = 0.1$ with small random noise. This state is a globally mixed state, as shown in the leftmost panels of Fig. 2(b). At $t = 0$, g_{12} is suddenly changed to 15.3 [the same condition as in Fig. 2(a)], and the mixed bubbles are dynamically formed by spinodal decomposition. In the Supplemental Material [33], collective excitation of a single bubble is also provided.

For $U = 1$, the energy curve acquires the shape shown in Fig. 1(c) (curve II). Around $C = 0.5$, the energy curve is convex, and therefore the globally mixed state is stable against a small change in C ($|C_\pm - C_0| \ll 1$). However, the true ground state is the totally separated phases with $C = 0$ and $C = 1$, and the globally mixed state with $C \simeq 0.5$ is a metastable state. Figures 3(a) and 3(b) show the dynamics that start from the metastable state with $C = 0.5$, where a local perturbation potential $Ae^{-(x^2+y^2)/2}$ for component 1 is switched on at $t = 0$ to trigger the nucleation. Figure 3(a) shows the case of $A = 1$; the phase separation is triggered around the center by the perturbation potential, and the concentric phase separation extends outward. In the case of a smaller perturbation ($A = 0.05$), as shown in Fig. 3(b), the density distributions around the center are slightly modified by the perturbation potential, which is insufficient

to trigger the phase separation. This corroborates the existence of an energy barrier against nucleation.

Figure 4(a) depicts the stability of the globally mixed state with respect to C and U. For the region in which the energy curve $\varepsilon(C)$ is concave, $\partial^2\varepsilon/\partial C^2 < 0$, the globally mixed state is unstable against phase separation, and the inflection points [circles in Fig. 4(b) for $U = 1.2$] trace the spinodal curve in Fig. 4(a). For $U \lesssim 0.94$, $\varepsilon(C)$ is concave everywhere, and there are no inflection points. The tangential lines, as shown in Fig. 4(b), give the mixed-bubble states, and a globally mixed state for C between the square and triangle in Fig. 4(b) has higher energy than the mixed-bubble state. Therefore, the region between the circle and triangle is metastable. For $U \simeq 1.1$, the states with $C = 0$, $C = 0.5$, and $C = 1$ become degenerate [curve III in Fig. 1(c)], and these three phases (occupied only by component 1 or 2, or equally mixed) can coexist.

Experimentally, the phenomena presented here can be realized by a two-component BEC with scattering lengths that satisfy the immiscible condition $a_{12}^2 - a_{11}a_{22} > 0$. (See the Supplemental Material [33] for an example of an experimental system.) A boxlike potential rather than a harmonic potential is suitable to avoid the complexity
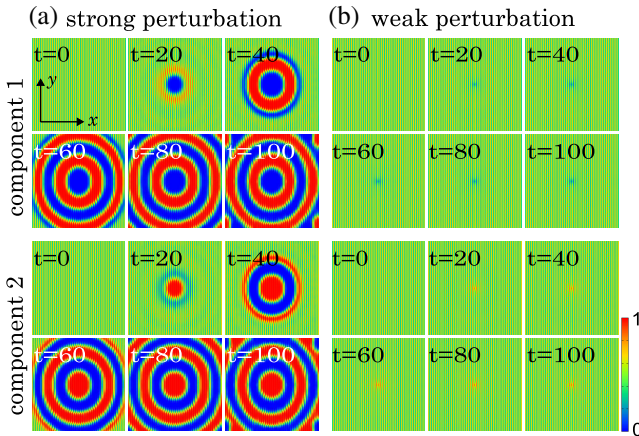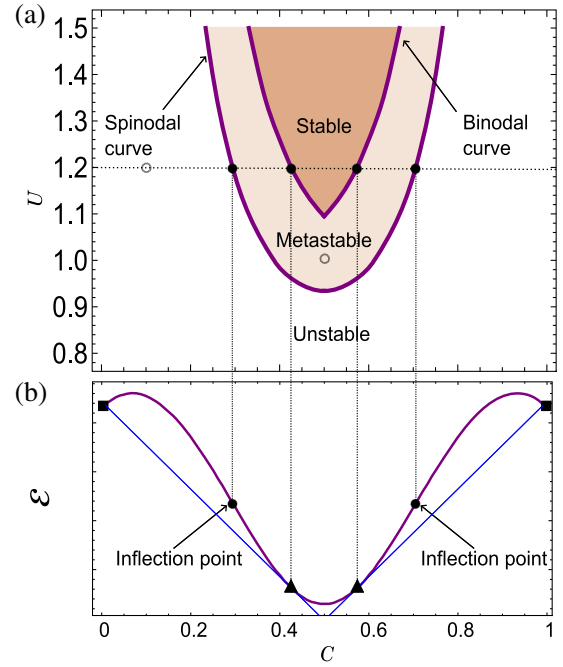
FIG. 3. Dynamics for $C = 0.5$, $g = 15$, $g_{12} = 15.3$, and $U = 1$. The energy curve for these parameters is shown in Fig. 1(c) (curve II). The initial state is the metastable state with $C = 0.5$ (circle on curve II). At $t = 0$, a local perturbation potential $Ae^{-(x^2+y^2)/2}$ is added to component 1 with (a) $A = 1$ and (b) $A = 0.05$. The size of each panel is $(64\pi)^2$ with the origin at the center. See the Supplemental Material [33] for movies of the dynamics.

FIG. 4. (a) Stability of the globally mixed state with respect to the composition C and potential strength U, where $g = 15$ and $g_{12} = 15.3$. The spinodal (binodal) curve divides the unstable (stable) and metastable regions. The parameters used in Figs. 2 and 3 are marked by the open circles. (b) Energy curve $\varepsilon(C)$ for $U = 1.2$. The inflection points (filled circles) trace the spinodal curve in (a). The tangent points (squares and triangles) give the mixed-bubble states. The points marked by the triangles trace the binodal curve in (a).

that arises from inhomogeneous density. A quasi-two-dimensional (or one-dimensional) system is convenient to observe the spatial density pattern, and also to suppress the total number of atoms; however, the dimensionality is not crucial for the present phenomena.

In conclusion, we have proposed a method to control the mixing properties of two fluids. The mixing energy can be changed by modulating the densities on a small scale using component-dependent external potentials, which alters the global mixing properties. This method was applied to a two-component BEC of dilute gases. Although this system originally has a trivial mixing property, the energy curve acquires a concave-convex shape with respect to the composition C by the present method, and spinodal and binodal physics emerge. As a result, the mixed-bubble state (Fig. 2), which has only been predicted for a system with quantum fluctuation, becomes possible within simple mean-field theory. The modification of the energy curve also results in a metastable state that undergoes phase separation via nucleation due to a finite local perturbation (Fig. 3). The present method is not restricted to quantum fluids and may also be applied to classical immiscible fluids, such as oil and water.

Appendix: The concave-convex energy curve.—To understand the underlying physics of the concave-convex energy curve in Fig. 1(c), we study the parameter dependence of the modulation amplitudes a_1 and a_2 in the variational function in Eq. (2). Figures 5(a) and 5(b) show the values of a_1 and a_2 that minimize the variational energy. For $C \simeq 0.5$, both a_1 and a_2 increase to large values (negative and positive) with U, which indicates that both components are well modulated by the periodic potential [see panel C of Fig. 1(d)]. On the other hand, when $C \simeq 0$, i.e., component 2 is dominant, a_2 remains small, as shown in Fig. 5(b), and the two components are not strongly modulated [see panel B of Fig. 1(d)]. This is because the total density tends to remain uniform due to the large chemical potential; if a_2 became large, the total density would be modulated at a high energy cost, because the modulation of component 2 (major component) cannot be compensated by that of component 1 (minor component). A similar argument applies to a_1 for $C \simeq 1$. As a result, $|a_1 a_2|$ can become large for $C \simeq 0.5$ and remains small for $C \simeq 0$ and $C \simeq 1$, as shown in Fig. 5(c). The energy valley in Fig. 1(b) originates from the behavior of Fig. 5(c) through the intercomponent interaction energy that includes $a_1 a_2$ [see the last term of Eq. (3)], resulting in the convex part of the energy curve. The concave part of
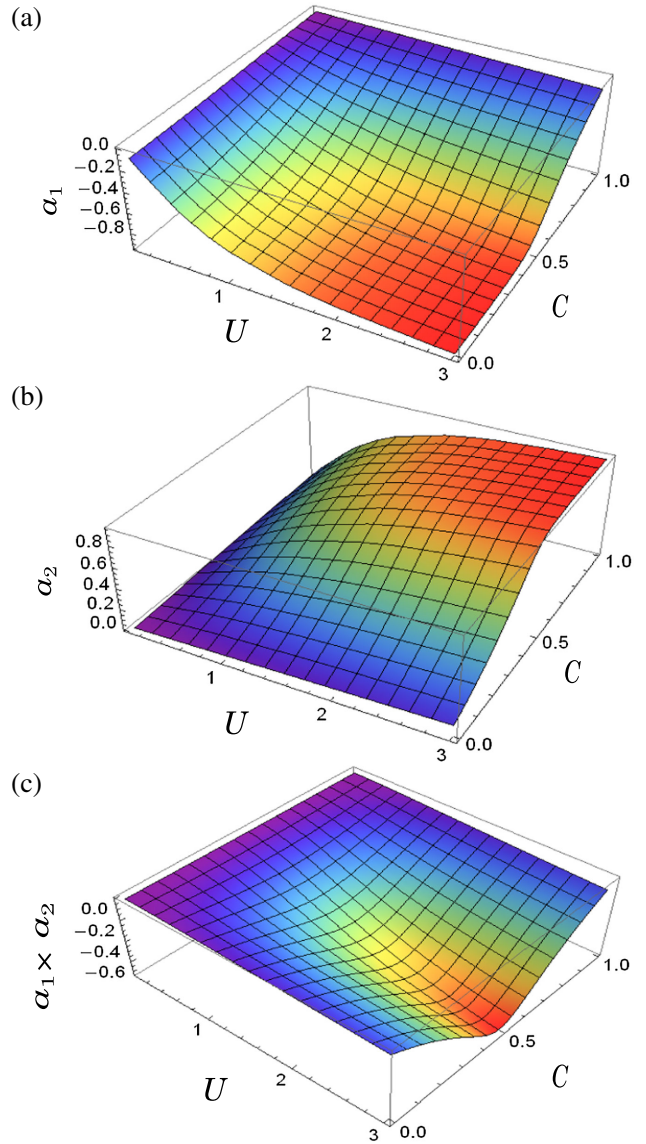

FIG. 5. Modulation amplitudes a_1 and a_2 in Eq. (2) that minimize the variational energy in Eq. (3), as functions of the potential strength U and composition C. The interaction parameters are the same as those in Fig. 1.

the energy curve originates from the usual immiscible interaction energy that does not include a_j. Thus, the concave-convex curve results from the competition between these energies.

[1] J. W. Cahn, On spinodal decomposition, Acta Metall. **9,** 795 (1961).

[2] J. W. Cahn, Phase separation by spinodal decomposition in isotropic systems, J. Chem. Phys. **42,** 93 (1965).

[3] J. S. Langer, M. Baron, and H. D. Miller, New computational method in the theory of spinodal decomposition, Phys. Rev. A **11,** 1417 (1975).

[4] E. P. Favvas and A. Ch. Mitropoulos, What is spinodal decomposition?, J. Eng. Sci. Technol. Rev. **1**, 25 (2008).

[5] D. W. Oxtoby, Homogeneous nucleation: Theory and experiment, J. Phys. Condens. Matter **4**, 7627 (1992).

[6] P. G. Debenedetti, *Metastable liquids: Concepts and Principles* (Princeton University Press, Princeton, NJ, 1997).

[7] D. Kashchiev, *Nucleation* (Elsevier, New York, 2000).

[8] C. J. Myatt, E. A. Burt, R. W. Ghrist, E. A. Cornell, and C. E. Wieman, Production of two overlapping Bose-Einstein condensates by sympathetic cooling, Phys. Rev. Lett. **78**, 586 (1997).

[9] D. S. Hall, M. R. Matthews, J. R. Ensher, C. E. Wieman, and E. A. Cornell, Dynamics of component separation in a binary mixture of Bose-Einstein condensates, Phys. Rev. Lett. **81**, 1539 (1998).

[10] G. Modugno, M. Modugno, F. Riboli, G. Roati, and M. Inguscio, Two atomic species superfluid, Phys. Rev. Lett. **89**, 190404 (2002).

[11] B. D. Esry, C. H. Greene, J. P. Burke, Jr., and J. L. Bohn, Hartree-Fock theory for double condensates, Phys. Rev. Lett. **78**, 3594 (1997).

[12] H. Pu and N. P. Bigelow, Properties of two-species Bose condensates, Phys. Rev. Lett. **80**, 1130 (1998).

[13] E. Timmermans, Phase separation of Bose-Einstein condensates, Phys. Rev. Lett. **81**, 5718 (1998).

[14] P. Ao and S. T. Chui, Binary Bose-Einstein condensate mixtures in weakly and strongly segregated phases, Phys. Rev. A **58**, 4836 (1998).

[15] M. Trippenbach, K. Góral, K. Rzazewski, B. Malomed, and Y. B. Band, Structure of binary Bose-Einstein condensates, J. Phys. B **33**, 4017 (2000).

[16] J. Catani, L. De Sarlo, G. Barontini, F. Minardi, and M. Inguscio, Degenerate Bose-Bose mixture in a three-dimensional optical lattice, Phys. Rev. A **77**, 011603(R) (2008).

[17] D. S. Petrov, Quantum mechanical stabilization of a collapsing Bose-Bose mixture, Phys. Rev. Lett. **115**, 155302 (2015).

[18] P. Naidon and D. S. Petrov, Mixed bubbles in Bose-Bose mixtures, Phys. Rev. Lett. **126**, 115301 (2021).

[19] P. Stürmer, M. N. Tengstrand, and S. M. Reimann, Mixed bubbles in a one-dimensional Bose-Bose mixture, Phys. Rev. Res. **4**, 043182 (2022).

[20] Q. Gu and X. Cui, Liquid-gas transition and coexistence in ground-state bosons with spin twist, Phys. Rev. A **107**, L031303 (2023).

[21] L. He, H. Li, W. Yi, and Z. Q. Yu, Quantum criticality of liquid-gas transition in a binary Bose mixture, Phys. Rev. Lett. **130**, 193001 (2023).

[22] G. Spada, S. Pilati, and S. Giorgini, Attractive solution of binary Bose mixtures: Liquid-vapor coexistence and critical point, Phys. Rev. Lett. **131**, 173404 (2023).

[23] C. J. Pethick and H. Smith, *Bose-Einstein Condensation in Dilute Gases*, 2nd ed. (Cambridge University Press, Cambridge, England, 2008).

[24] L. P. Pitaevskii and S. Stringari, *Bose-Einstein Condensation and Superfluidity* (Oxford University Press, New York, 2016).

[25] O. Mandel, M. Greiner, A. Widera, T. Rom, T. W. Hänsch, and I. Bloch, Coherent transport of neutral atoms in spin-dependent optical lattice potentials, Phys. Rev. Lett. **91**, 010407 (2003).

[26] L. J. LeBlanc and J. H. Thywissen, Species-specific optical lattices, Phys. Rev. A **75**, 053612 (2007).

[27] B. Gadway, D. Pertot, R. Reimann, and D. Schneble, Superfluidity of interacting bosonic mixtures in optical lattices, Phys. Rev. Lett. **105**, 045303 (2010).

[28] B. Arora, M. Safronova, and C. W. Clark, Tune-out wavelengths of alkali-metal atoms and their applications, Phys. Rev. A **84**, 043401 (2011).

[29] K. Wen, Z. Meng, L. Wang, L. Chen, L. Huang, P. Wang, and J. Zhang, Experimental study of tune-out wavelengths for spin-dependent optical lattice in ^{87}Rb Bose-Einstein condensation, J. Opt. Soc. Am. B **38**, 3269 (2021).

[30] Z. Meng, L. Wang, W. Han, F. Liu, K. Wen, C. Gao, P. Wang, C. Chin, and J. Zhang, Atomic Bose-Einstein condensate in twisted-bilayer optical lattices, Nature (London) **615**, 231 (2023).

[31] J. H. Kim, D. Hong, and Y. Shin, Observation of two sound modes in a binary superfluid gas, Phys. Rev. A **101**, 061601(R) (2020).

[32] J. H. Kim, D. Hong, K. Lee, and Y. Shin, Critical energy dissipation in a binary superfluid gas by a moving magnetic obstacle, Phys. Rev. Lett. **127**, 095302 (2021).

[33] See Supplemental Material at http://link.aps.org/supplemental/10.1103/PhysRevLett.132.173402, which includes Refs. [33–35], for additional information about the nondimensionalization, energy diagram, collective excitation of the bubble, and experimental proposal. The Supplemental Material also includes movies showing the dynamics of the system.

[34] Lord Rayleigh, On the capillary phenomena of jets, Proc. R. Soc. London **29**, 71 (1879).

[35] S. Knoop, T. Schuster, R. Scelle, A. Trautmann, J. Appmeier, and M. K. Oberthaler, Feshbach spectroscopy and analysis of the interaction potentials of ultracold sodium, Phys. Rev. A **83**, 042704 (2011).

[36] H.-J. Miesner, D. M. Stamper-Kurn, J. Stenger, S. Inouye, A. P. Chikkatur, and W. Ketterle, Observation of metastable states in spinor Bose-Einstein condensates, Phys. Rev. Lett. **82**, 2228 (1999).

[37] For the present parameters, the chemical potential is $\simeq 15$, while the height of the periodic potential is ~ 1, and the system is far from the tight-binding regime.

[38] G.-R. Jin, C. K. Kim, and K. Nahm, Modulational instability of two-component Bose-Einstein condensates in an optical lattice, Phys. Rev. A **72**, 045601 (2005).

[39] T. Roscilde and J. I. Cirac, Quantum emulsion: A glassy phase of bosonic mixtures in optical lattices, Phys. Rev. Lett. **98**, 190402 (2007).

[40] J. Ruostekoski and Z. Dutton, Dynamical and energetic instabilities in multicomponent Bose-Einstein condensates in optical lattices, Phys. Rev. A **76**, 063607 (2007).

[41] P. Buonsante, S. M. Giampaolo, F. Illuminati, V. Penna, and A. Vezzani, Mixtures of strongly interacting bosons in optical lattices, Phys. Rev. Lett. **100**, 240402 (2008).

[42] M. M. Maśka, R. Lemański, J. K. Freericks, and C. J. Williams, Pattern formation in mixtures of ultracold atoms in optical lattices, Phys. Rev. Lett. **101**, 060404 (2008).

[43] U. Shrestha, J. Javanainen, and J. Ruostekoski, Pulsating and persistent vector solitons in a Bose-Einstein condensate in a lattice upon phase separation instability, Phys. Rev. Lett. **103**, 190401 (2009).

[44] P. Buonsante, S. M. Giampaolo, F. Illuminati, V. Penna, and A. Vezzani, Unconventional quantum phases in lattice bosonic mixtures, Eur. Phys. J. B **68**, 427 (2009).

[45] J.-J. Wang, A.-X. Zhang, K.-Z. Zhang, J. Ma, and J.-K. Xue, Two-component Bose-Einstein condensates in D-dimensional optical lattices, Phys. Rev. A **81**, 033607 (2010).

[46] T. Ozaki and T. Nikuni, Phase separation in Bose-Bose mixtures in an optical lattice, J. Phys. Soc. Jpn. **81**, 024001 (2012).

[47] K. Suthar and D. Angom, Characteristic temperature for the immiscible-miscible transition of binary condensates in optical lattices, Phys. Rev. A **95**, 043602 (2017).

[48] D. A. Porter, K. E. Easterling, and M. Sherif, *Phase Transformation in Metals and Alloys*, 4th ed. (CRC Press, Boca Raton, 2021).

[49] W. H. Press, S. A. Teukolsky, W. T. Vetterling, and B. P. Flannery, *Numerical Recipes*, 3rd ed. (Cambridge University Press, Cambridge, England, 2007).